

## OPTICAL DISPERSION RELATIONS FOR "DIAMONDLIKE" CARBON FILMS

Samuel A. Alterovitz\*, Robert M. Sieg†, Neil S. Shoemaker‡, and  
John J. Pouch\*

\*NASA Lewis Research Center, Cleveland, Ohio 44135

†Undergraduate Student Intern at NASA Lewis Research Center from Cleveland,  
State University, Dept. of Electrical Engineering, Cleveland, Ohio 44106

‡Undergraduate Student Intern at NASA Lewis Research Center from Case  
Western Reserve University, Physics Dept., Cleveland, Ohio 44115

### ABSTRACT

Ellipsometric measurements on plasma deposited "diamondlike" amorphous carbon (a-C:H) films were taken in the visible, ( $E = 1.75$  to  $3.5$  eV). The films were deposited on Si and their properties were varied using high temperature (up to  $750$  °C) anneals. The real ( $n$ ) and imaginary ( $k$ ) parts of the complex index of refraction  $N$  were obtained simultaneously. Following the theory of Forouhi and Bloomer (Phys. Rev. B34, 7018 (1986)), a least squares fit was used to find the dispersion relations  $n(E)$  and  $k(E)$ . Reasonably good fits were obtained, showing that the theory can be used for a-C:H films. Moreover, the value of the energy gap  $E_g$  obtained in this way was compared to the  $E_g$  value using conventional Tauc plots and reasonably good agreement was obtained.

### INTRODUCTION

The optical energy band gap of amorphous materials is usually found using a Tauc plot [1], i.e., an extrapolation of  $(\alpha n E)^{1/2}$  versus  $E$ . Here  $\alpha$  is the optical absorption coefficient,  $n$  is the refractive index and  $E$  is the energy. In many cases, the refractive index is almost constant or is unavailable, and  $(\alpha E)^{1/2}$  versus  $E$  is used (simplified Tauc). There are several drawbacks to the Tauc theory and procedure. First, the theory relates to absorption only, and cannot give the refractive index through the Kramers-Kronig relation [2]. Second, there is ambiguity on the energy range that the Tauc extrapolation is correct. Below a certain value of  $\alpha$ , the absorption falls exponentially. This regime is called the Urbach edge [1]. The onset for this regime varies and values of order  $\alpha = 10^3$  cm<sup>-1</sup> [1] up to  $\alpha = 10^4$  cm<sup>-1</sup> [3] have been used. Empirically, many Tauc plots also start to deviate from a straight line at high  $\alpha$  values [4,5].

Recently, an extension of the theory of optical absorption has been published for amorphous materials [2]. Later, the theory was extended to include more than one critical point, and was applied to crystalline semiconductors [6]. In the Tauc plot derivation [1], the main assumptions are a constant matrix element and parabolic density of states for both the valence and the conduction bands. However, if the excited state has a finite lifetime  $\tau$ , the absorption probability has a damping factor [2] and Tauc plots are theoretically incorrect. The extinction coefficient  $k$  ( $k = \alpha \hbar / 2E$  where  $E$  is the energy) is calculated in [2,6] using the lifetime concept, obtaining.

$$k(E) = \frac{A(E - E_g)^2}{E^2 - BE + C} \quad (1)$$

Here  $A$  is  $k(\infty)$  and is proportional to  $M^2/\tau$  where  $M$  is the position matrix element ( $M = \langle f|x|i \rangle$ );  $B = 2(E_{c,crit} - E_{v,crit})$ , where  $E_{c,crit}$  and  $E_{v,crit}$  are energies in the conduction and valence band respectively corresponding to a critical point, i.e., where  $k(E_{c,crit} - E_{v,crit})$  is a maximum.  $C$  is related to the lifetime  $\tau$  through  $\hbar/\tau = (4C - B^2)^{1/2}$  and

$E_g = E_{c, \text{bottom}} - E_{v, \text{top}}$ , i.e., the optical bandgap. Using the Kramers-Kronig relation, the refractive index was obtained [2]:

$$n(k) = n(\infty) + \frac{B_0 E + C_0}{E^2 - BE + C} \quad (2)$$

Here  $B_0$  and  $C_0$  are related to  $A, B$  and  $C$  through simple algebraic formulas, and  $n(\infty)$  is a constant.

In this paper we will examine if this new result applies to "diamond-like" carbon, also denoted a-C:H (amorphous hydrogenated carbon). If applicable, the result can give the  $n(E)$  function from a known absorption spectrum  $k(E)$  and a single refractive index measurement. Also, the functions  $n(E)$  and/or  $k(E)$  can be used when their analytical form is required, e.g., optimizing antireflection filters. In addition, this paper will discuss the meaning of the experimental constants,  $A, B, C$ , and  $E_g$ .

Amorphous hydrogenated carbon material is made almost exclusively in form of thin films. The natural choice for an experimental technique is ellipsometry. The multiple angle of incidence, multiple wavelengths (MAW) technique [7 to 9] was used. MAW gives  $n$  and  $k$  of the film simultaneously at all wavelengths measured, without the use of either a known dispersion relation or application of the Kramers-Kronig analysis. This technique was commonly used to analyze various semiconductor multilayer structures [10,11] when  $n$  and  $k$  of the constituents were known. Here, the MAW technique is used in a spectroscopic way, to measure unknown  $n(E)$  and  $k(E)$ . The smallest value of  $k$  that is accurately determined by ellipsometry is of order 0.005, corresponding to  $\alpha \approx 1000 \text{ cm}^{-1}$  in the visible. Thus, the Urbach edge regime is almost eliminated from this work. Reflection ellipsometry has the added benefit of measuring the thin film samples on any substrate, in contrast to transmission experiments. As the optical energy bandgap  $E_g$  depends on the substrate material [5], possibly due to differences in conductivity, this advantage of ellipsometry can be crucial for actual applications.

## EXPERIMENTAL

Samples were prepared on 3 in. diameter Si substrates using a 30 kHz plasma deposition unit. The power  $P$  used was in the range 50 to 200 W, with a constant flow rate of  $7 \times 10^{-5} \text{ m}^3/\text{min}$ . Details of the growth chamber are given in [12]. Several samples cut from the 150 W wafer were annealed in nitrogen for 10 sec using a rapid thermal anneal module [5]. The rotating analyzer ellipsometer set-up [13] is essentially similar to the one described in [10]. At each angle of incidence, data was taken in the wavelength range 3500 to 7300 Å, with 100 Å intervals. Five angles of incidence were used, usually in the range  $55^\circ$  to  $75^\circ$ . Each measurement consisted of 100 rev, with 72 points per rev, taken at a rate of  $\sim 50 \text{ rev/sec}$ . Background subtraction was done at each point. Calibration of the absolute value of the ellipsometric parameters  $\psi$  and  $\Delta$  was done using [14]. The double grating monochromator was controlled by a IBM-AT personal computer that was also used for all data acquisition and analysis.  $\psi$  and  $\Delta$  were obtained by Fourier analysis. The MAW inversion process was done by minimizing experimental  $\psi$  and  $\Delta$  (or  $\tan \psi$  and  $\cos \Delta$ ) versus their calculated values [9]. The model used included only the substrate and a homogeneous film. This is a reasonable approximation, as the interface of a-C:H on Si includes only the native oxide and  $\sim 5 \text{ \AA}$   $\text{SiC}_x$  [15], and our films were above 1000 Å thick.

## RESULTS

Seven samples were measured. Simplified and regular Tauc plots were done for all samples. A representative plot (50 W sample) is given in

Fig. 1, showing a slightly concave result versus the theory. As the annealing temperature and/or deposition power rises, the experimental Tauc function first becomes a straight line and later turns convex. We kept the extrapolation range to the linear part of the experimental function. A summary of the energy bandgaps obtained from regular and simplified Tauc plots, together with sample thicknesses  $t$ , are given in Table I. Results of  $n(E)$  and  $k(E)$  for the 50 and 150 W, 600 °C samples are given in Figs 2 and 3 respectively. Figure 2 shows a rising  $n$  versus  $E$  while Fig. 3 show a decreasing  $n(E)$ . All other samples have an interim type of behavior. Grid least square fits to Eq. (1) were done to obtain A,B,C and  $E_g$  simultaneously. With these 4 parameters fixed, the value of  $n(\infty)$  was set to get the best  $n(E)$  fits. The solid lines in Figs. 2 and 3 were calculated using these parameters. Results for all samples are given in Table II, while  $E_g$  is also displayed in Table I.

TABLE I a-C:H OPTICAL ENERGY GAPS IN eV

P, W	T, °C	t, Å	Sqrt( $\alpha E$ )	Sqrt( $\alpha E n$ )	Grid
50	-	1490	1.90	1.90	1.64
100	-	2305	2.65	2.65	2.70
150	-	2810	2.36	2.36	2.23
200	-	2960	2.02	2.02	1.65
150	400	2560	2.05	2.06	1.90
150	600	1320	1.08	0.89	1.03
150	750	950	0.57	0.39	0.39

TABLE II DISPERSION RELATION PARAMETERS FOR a-C:H FILMS

P, W	T, C	A	B, eV	C, (eV) <sup>2</sup>	$E_g$ , eV	$n(\infty)$
50	-	.06	6.39	12.67	1.64	1.63
100	-	.01	6.46	10.51	2.70	1.70
150	-	.05	5.90	9.75	2.23	1.67
200	-	.11	5.99	11.73	1.65	1.69
150	400	.06	5.10	7.20	1.90	1.70
150	600	.40	3.66	4.22	1.03	1.58
150	750	.85	1.21	1.85	0.39	1.71

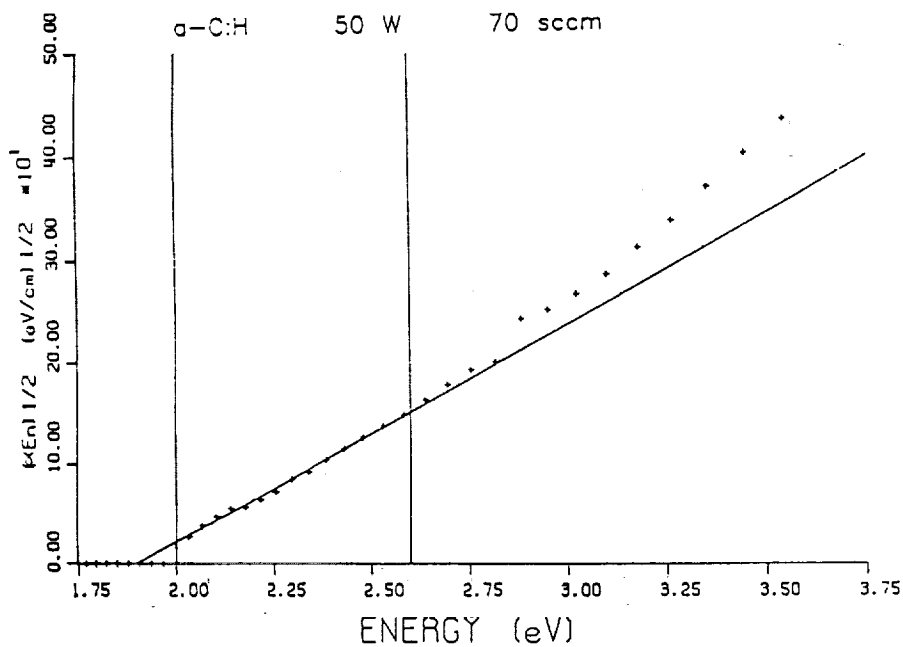


FIGURE 1. TAUC PLOT FOR THE 50 W SAMPLE. VERTICAL LINES SHOW THE FITTING RANGE.

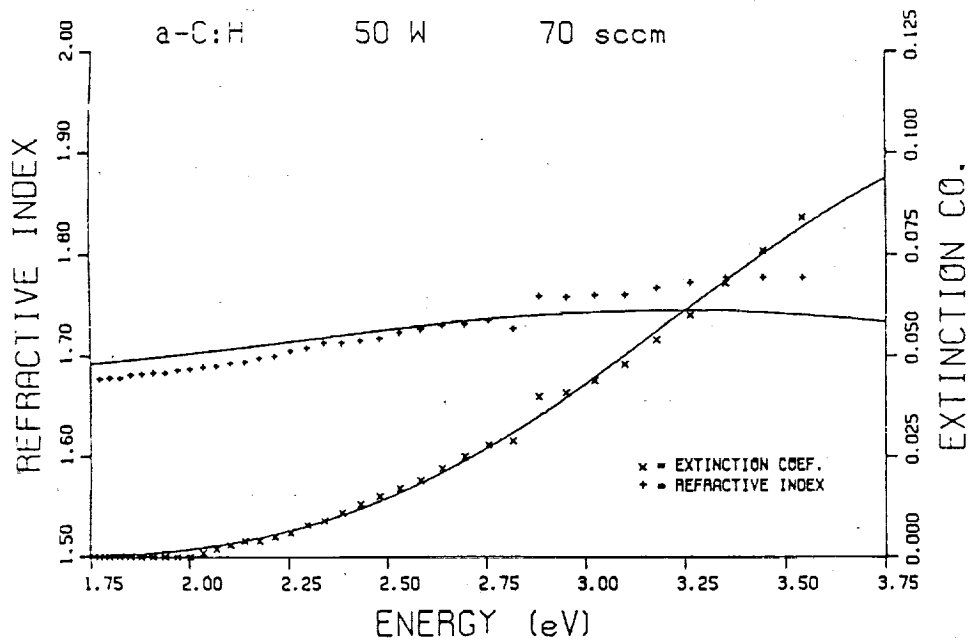


FIGURE 2. REFRACTIVE INDEX AND EXTINCTION COEFFICIENT OF THE 50 W SAMPLE. SOLID LINES ARE DUE TO EQUATIONS (1) AND (2).

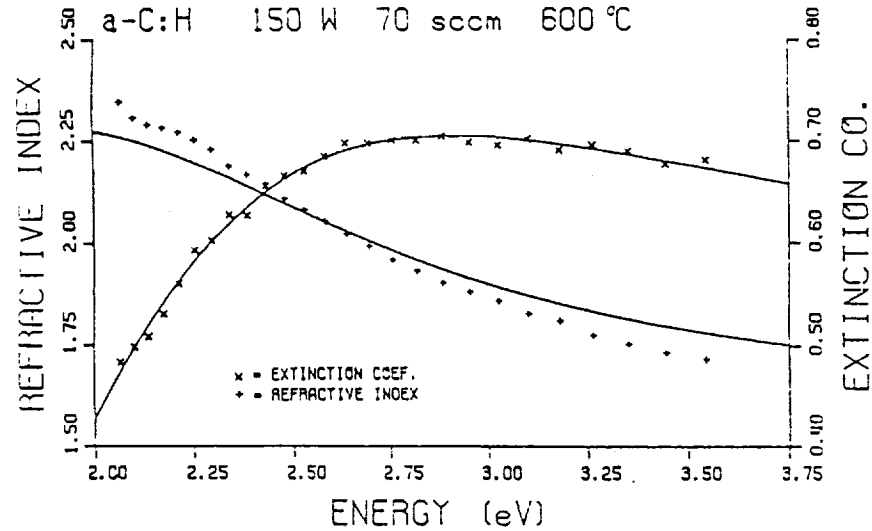


FIGURE 3. REFRACTIVE INDEX AND EXTINCTION COEFFICIENT OF THE 150 W, 600 °C SAMPLE. SOLID LINES ARE DUE TO EQUATIONS (1) AND (2).

#### DISCUSSION

Optical energy bandgaps  $E_g$  found using the two Tauc procedures are identical. However,  $E_g$  found using the dispersion relation fits are almost always smaller than the Tauc plots, although the differences are not very large. It is impossible to rule which bandgap is the "correct" one. The dispersion relation functions do take into account, at least qualitatively, the existence of absorption at lower energy than the regular Tauc regime, the Urbach tail. This can be seen by the very small slope of  $k(E)$  near  $E_g$ , as shown in Fig. 2. However,  $\alpha(E)$  is expected to be purely exponential in the Urbach edge [1]. Thus, theoretically, the dispersion relations do not describe this regime. Table I also shows a decrease in  $E_g$  with increasing deposition power, (except the 50 W sample) and with increasing annealing temperature, in agreement with prior results [4,5]. The thickness increases with power [16] and decreases with annealing temperature.

The quality of the fits shown in Figs. 2 and 3 is quite good. The  $n(E)$  fits are the real test of the theory and the figures show a reasonable agreement between experiment and calculation. All other  $n(E)$  experimental curves show an equal or better fit to theory, as they include almost constant  $n(E)$  values. In addition, the  $k(E)$  fit is definitely better than the Tauc fits.

The value of the A,B,C parameters, as shown in Table II, are essentially constant as function of deposition power, but they change significantly versus annealing temperature. The value of the lifetime  $\hbar/\tau$ , deduced from  $(4C - B^2)^{1/2}$ , has quite an amount of scatter. However, all results are around  $\hbar/\tau \approx 2$  eV. This is a large value, but it is comparable with other amorphous materials [2]. The values of A are in general lower than for other materials [2], denoting a smaller position matrix element M in a-C:H. There is an order of magnitude increase in M with heating to 750 °C. It would be interesting to correlate this increase with the changes in the composition and crystallivity of a-C:H. The value of B for the room temperature deposited samples, is equal to the lowest values obtained for other materials [2], and drops markedly with annealing temperature. The value of  $B/2$  is characteristic of the critical point bandgap [6], denoting a sharp decrease in this bandgap, in parallel with the sharp  $E_g$  drop. However, we did not see signs of a peak in  $k(E)$  at  $E = B/2$ , as expected for a critical point.

## CONCLUSION

Dispersion relations suggested in [2] are obeyed, although the  $n(E)$  function does not have a perfect fit. Values of the parameters for the bandgaps  $B$  and  $E_g$  show reasonable agreement with  $\tau_{\text{auc}}$  plots and with prior results. The position matrix element increases with increasing annealing temperature.

## REFERENCES

1. N.F. Mott and E.A. Davis, Electronic Processes in Non-Crystalline Materials, 2nd ed. (Clarendon Press, Oxford, 1979).
2. A.R. Forouhi and I. Bloomer, Phys. Rev. B, 34, 7018 (1986).
3. J. Robertson, Adv. Phys., 35, 317 (1986).
4. S.A. Alterovitz, J.D. Warner, D.C. Liu and J.J. Pouch, J. Electrochem. Soc., 133, 2339 (1986).
5. S.A. Alterovitz, J.J. Pouch and J.D. Warner, in Rapid Thermal Processing of Electronic Materials, edited by S.R. Wilson, R. Powell, and D.E. Davies, (Mater. Res. Soc. Proc. 92, Pittsburgh, PA, 1987) pp. 311-318.
6. A.R. Forouhi and I. Bloomer, Phys. Rev. B, 38, 1865 (1988).
7. S.A. Alterovitz, G.H. Bu-Abbud, J.A. Woollam, and D.C. Liu, J. Appl. Phys., 54, 1559 (1983).
8. G.H. Bu-Abbud, S.A. Alterovitz, N.M. Bashara and J.A. Woollam, J. Vac. Sci. Technol., A, 1, 619 (1983).
9. G.H. Bu-Abbud, N.M. Bashara, and J.A. Woollam, Thin Solid Films, 133, 27 (1986).
10. P.G. Snyder, M.C. Rost, G.H. Bu-Abbud, J.A. Woollam, and S.A. Alterovitz, J. Appl. Phys., 60, 3293 (1986).
11. S.A. Alterovitz, J.A. Woollam, and P.G. Snyder, Sol. State Tech., 31 (3), 99 (1988).
12. J.J. Pouch, J.D. Warner, D.C. Liu and S.A. Alterovitz, Thin Solid Films, 157, 97 (1988).
13. J.A. Woollam Co., Lincoln, NB.
14. D.E. Aspnes and A.A. Studna, Appl. Opt., 14, 220 (1975).
15. R.W. Collins, Appl. Phys. Lett., 52, 2025 (1988).
16. J.J. Pouch, S.A. Alterovitz, J.D. Warner, D.C. Liu, and W.A. Lanford, in Thin Films: The Relationship of Structure to Properties, edited by C.R. Aita and K.S. Sreeharsha, (Mater. Res. Soc. Proc. 47, Pittsburgh, PA, 1985) pp. 201-204.